SILESIAN UNIVERSITY OF TECHNOLOGY PUBLISHING HOUSE

SCIENTIFIC PAPERS OF SILESIAN UNIVERSITY OF TECHNOLOGY 2023
ORGANIZATION AND MANAGEMENT SERIES NO. 186

A NEW APPROACH TO PREPROCESSING OF EMG SIGNAL TO ASSESS THE CORRECTNESS OF MUSCLE CONDITION

Dariusz KOMOROWSKI[1*], Barbara MIKA[2], Piotr KACZMAREK[3]

[1] Silesian University of Technology, Faculty of Biomedical Engineering; dariusz.komorowski@polsl.pl, ORCID: 0000-0003-4430-6047
[2] Silesian University of Technology, Faculty of Biomedical Engineering; barbara.mika@polsl.pl, ORCID: 0000-0001-7094-2405
[3] Poznan University of Technology, Institute of Robotics and Machine Intelligence; piotr.kaczmarek@put.poznan.pl, ORCID: 0000-0002-0625-3960)
* Correspondence author

Purpose: Electromyography (EMG) is a technique dealing with the recording and analysis of myoelectric signals formed by physiological variations in the muscle fiber membrane. The voltage potential of surface myoelectrical signals (sEMG) varies over time and depends on the characteristics of the individual subject. One of the main drawbacks of sEMG analysis is that the given acquisition conditions strongly determine the amplitude of the signal. The analysis of sEMG requires appropriate preprocessing, including proper filtering and artifact removal. Moreover, the sEMG data must be converted to a scale standardized for all measurements. This research aimed both to propose a method of sEMG processing to eliminate the occurring disturbances, in particular impulsive artifacts, and to determine the level of muscle excitation based on normalized sEMG. The analysis of muscle excitation level can be applied to assess muscle activity during physical activity.
Design/methodology/approach: The proposed algorithm uses set of digital filters, probabilistic distribution and the decomposition of the sEMG signal to attenuate artifacts. Variance analysis of the sEMG derivative is used to determine muscle excitation. The sEMG signals were acquired with the VICON system with the sampling frequency set at 1000 Hz, and processed in MATLAB. During sEMG recordings, standard silver/silver chloride (Ag/AgCl) surface electrodes were used.
Findings: The suggested technique was validated using sEMG recorded for eight persons during deep squat. Normalized excitation was determined for the left and right muscles, the rectus femoris, the vastus medialis, and the biceps femoris. Obtained outcomes indicate a possibility to assess the correctness of muscles condition.
Originality/value: The combination of the proposed filter and the analysis variance-based thresholding method can effectively eliminate impulse artifacts within the surface myoelectrical signals.

Keywords: Spikes disturbance, EMG, Muscle excitation, Filtering, Kurtosis.

Category of the paper: Research paper.

1. Introduction

Electromyography (EMG) is a technique that deals with, records, and analyzes myoelectrical signals formed by physiological variations in the state of sarcolemma – the muscle fiber membrane. The EMG signal is based upon action potentials that occur in the muscle fiber membrane as a consequence of depolarization and repolarization processes (De Luca, 1979). These rapid sequences of voltage changes in the sarcolemma induce the resulting excitation (electromechanical coupling) and finally cause a shortening of the contractile elements of the muscle cell manifested by muscle contraction (Konrad, 2005). Although excitation and contraction present a highly correlated relationship, it is known that weak excitation does not have to result in contractions (Konrad, 2005). The cell body, dendrites, and the motor neuron axon that innervates the bunch of muscle fibers is the smallest functional unit, so-called motor unit (motor neuron plus muscle fibers), of neural control of the muscular contraction process (Moritani et al., 2004; Staudenmann et al., 2010). The term unit is used because all muscle fibers within motor units behave and act as one in the innervation process. Methods used to measure these signals include surface EMG (sEMG), where electrodes are placed on the skin over the measured muscle, or intramuscular EMG (iEMG), where the electrodes are inserted through the skin into muscle tissue (Farina et al., 2016; Trontelj et al., 2004). The sEMG signal is a superposition of individual motor unit action potentials (MUAPs) within the pick-up range of the surface electrodes (Rodríguez-Carreño et al., 2012). Recruitment of MUAPs and their firing frequency could be pointed out as the major control action to adjust contraction and modulate the force output of the involved muscle (Konrad, 2005; Michell, 2013). Surface EMG is very attractive for researchers from various disciplines, such as medicine (Zwarts et al., 2004; Sadikoglu et al., 2017; Chmielewska et al., 2019; Jórasz et al., 2023; Wang et al., 2010; Martín et al., 2012; Merletti, Parker, 2004; Zieliński et al., 2022a, 2022b; Yin et al., 2020; Xu et al., 2022; Pilkar et al., 2020), sport or rehabilitation (Merletti, Parker, 2004; Yin et al., 2020; Xu et al., 2022; Pilkar et al., 2020) mainly since its significant constituents, motor unit recruitment, and rate coding, are also the precursors of active force generation (Staudenmann et al., 2010; Farina et al., 2002, 2016; Vigotsky et al., 2018). Muscle force production is preceded by excitation input from the central nervous system into the muscle. This signal triggers the excitation-contraction coupling, which leads to muscle activation (Dulhunty, 2006). Finally, muscle force is produced after cross-bridges are formed, and it is transmitted through the muscle (Zajac, 1989). With appropriate processing, sEMG can provide information on the timing and degree of muscle excitation and could be useful for providing insight into how the neuromuscular system behaves.

Muscles are the motors or brakes of locomotion, but they act reflexively, guided by the commands of the central nervous system (CNS) (Konrad, 2005). Muscle activation expresses an active contribution to muscle force and does not take into account passive components.

Furthermore, activation versus force production is not affected by fiber length and velocity. Activation reflects the number of fibers that are active, not the force-generating capacity of those fibers (Vigotsky et al., 2018). Because sEMG measures changes in the polarity of muscle fiber sarcolemma resulting from neural excitation, it could be accepted that sEMG is a measure of muscle excitation but not a direct measure of activation. Excitation precedes muscle activation (Zajac, 1989), so the existing relationship is reflected in sEMG. An unfiltered and unprocessed signal detecting the superposed MUAPs is called a raw sEMG. Raw sEMG is mostly affected by motor unit recruitment and rate coding. The envelope of this signal may be regarded as the sum of MUAPs of the sarcolemma of the area of muscle over which the electrode is located. Since raw sEMG is a complex signal, its processing, for example filtering, could provide data that are referred to muscle excitation (Vigotsky et al., 2018) and can be used to detect muscle fatigue (Sarillee et al., 2014; Calderón et al., 2014; Sun et al., 2022).

The aim of this paper is to propose a new approach to sEMG signal processing in order to eliminate the disturbances occurring in the surface electromyography signals (Chowdhury et al., 2013; de Luca et al., 2010), in particular, impulse artifacts and to determine the level of muscle excitation. The suggested method could enable an assessment of the muscle condition. The proposed approach focuses on determining the level of muscle activation in such a way as to eliminate the basic disadvantage of the standard method, in which the determined maximum excitation is usually based on the maximum or average value (Konrad, 2005) and can take into account the appearing impulse disturbances.

The paper is organized as follows. In the section Materials and Methods the detailed description of algorithm for preprocessing sEMG signal, in particular attenuation of impulse artifacts, and method of determining muscle excitation are provided. In the section Results, based on real sEMG signals recorded for eight athletes during deep squat, the proposed methods are used to determine the excitation of the rectus femoris, vastus medialis, and biceps femoris. Next, the results obtained are compared to the results provided by the chosen classical method and simple statistical analysis is performed for both sets of results. Finally, the outcomes are discussed in section Discussion.

2. Materials and Methods

This section introduces the method of preprocessing the sEMG signal, finding the signal envelope and threshold value connected to the muscle excitation. The calculated threshold corresponds to the maximum excitation value of the muscle. The paper presents the operation of the proposed method and an example of the results of research carried out on eight athletes during deep squat activity. The average age of surveyed athletes was 25.86 years (range: 23-29), and the average body max index (BMI) was 24.56 kg/m^2 (range: 22.7-26.3).

Each athlete gave their written consent to participate in the study. The sEMG signals were acquired with the VICON system with the sampling frequency set at 1000 Hz, and processed in MATLAB (R2021a). During sEMG recordings, standard silver/silver chloride (Ag/AgCl) surface electrodes were used. The electrodes had a Ag/AgCl disk with a diameter of about 7 mm. Therefore, the conductive surface was about 38 mm^2. The skin was rubbed with a mild abrasive to improve electrode-skin contact. The electrodes were placed according to SENIAM (Surface Electromyography for the Non-Invasive Assessment of Muscles) recommendations (Stegeman, Hermens, 2007). The SENIAM project is a European concerted action in the Biomedical Health and Research Program (BIOMED II) of the European Union. The SENIAM project developed important guidelines for EMG measurements that include, in particular, information on the characteristic and position of the electrodes (Hermens et al., 1999; Freriks, Hermens, 1999). All sessions with the recording of the sEMG signal took place in the first half of the day.

In our tests, participants (athletes) were asked to generate a maximum voluntary contraction for about 5 seconds, and this activity was repeated two times. The other exercises (deep squats) studied in this work were repeated twice in each trial. A kurtosis value calculated in the moving window was used to represent the quality of muscle excitation. For further analysis, the intervals of sEMG with kurtosis closer to 3 were taken to estimate MVC activity level (determined for selected muscle). The MVC-related activity was used for the normalization process performed for the sEMG signals recorded during deep squat exercises. Normalization was performed by dividing determined muscle excitation by the MVC value.

2.1. Surface EMG processing pipeline

The proposed method of sEMG processing consists of two main steps, that is, filtering and envelope calculation with threshold process. The sEMG processing pipeline is shown in Figure 1.

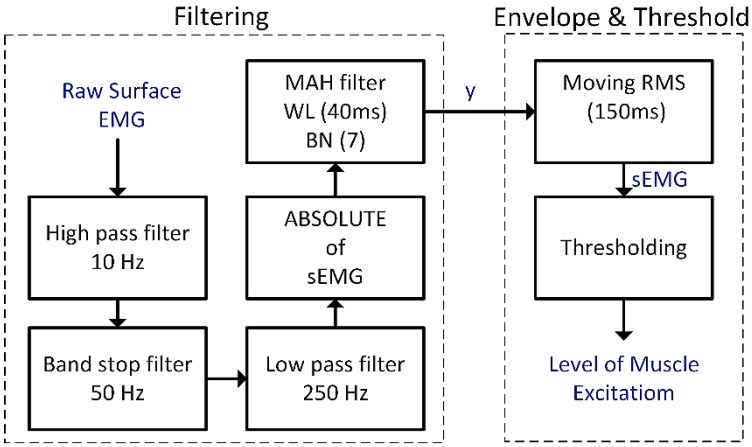

Figure 1. The block diagram with two main steps of the proposed sEMG processing method. The first: filtering with a set of dedicated digital filters, and the second: envelope calculation and threshold process.

This is due to the fact that the sEMG signal is weak and can present a lot of artifacts (Konrad, 2005; Reaz et al., 2006), the analysis of sEMG requires appropriate preprocessing, which includes proper filtering and artifact removal methods (Qiu et al., 2015; Yeon, Herr, 2021; Boyer et al., 2023). The sEMG signal is usually smoothed by a method based on the root mean square (RMS) calculation (Burden et al., 2014; Arabadzhiev et al., 2010; Gupta et al., 2017; Rose, 2014; Karabulut et al., 2017; Arozi et al., 2020; Josephson, Knight, 2019). RMS reflects the mean power of the signal (Luca, 1997). During the preprocessing stage, the EMG signal was filtering by three types of digital finite impulse response filters (FIR): the high pass filter (HPF) with a cutoff frequency set to 10 Hz (Stegeman, Hermens, 2007), the low pass filter (LPF) with a cutoff frequency set to 250 Hz, and the band stop filter (BSF) to suppress the mains interference (50 Hz). A moving average (Smith, 1997-1998; Kabe, Sako, 2020) hole filter (MAHF) slid a window of 2WL length (WL = 40 ms) along the sEMG data. The seven-bin histogram of the sEMG data contained in the window: X = {x[n], x[n − 1], ... x[n − (2WL − 1)]} was calculated. Then the vector D of the sEMG samples d[i], for i ∈ {k, k − 1..., (K − 1)}, where K < 2WL, belonging to the three most numerous bins, was created. The mean value of D is the output of the filter. The principle of the operation of MAHF is presented in Figure 2.

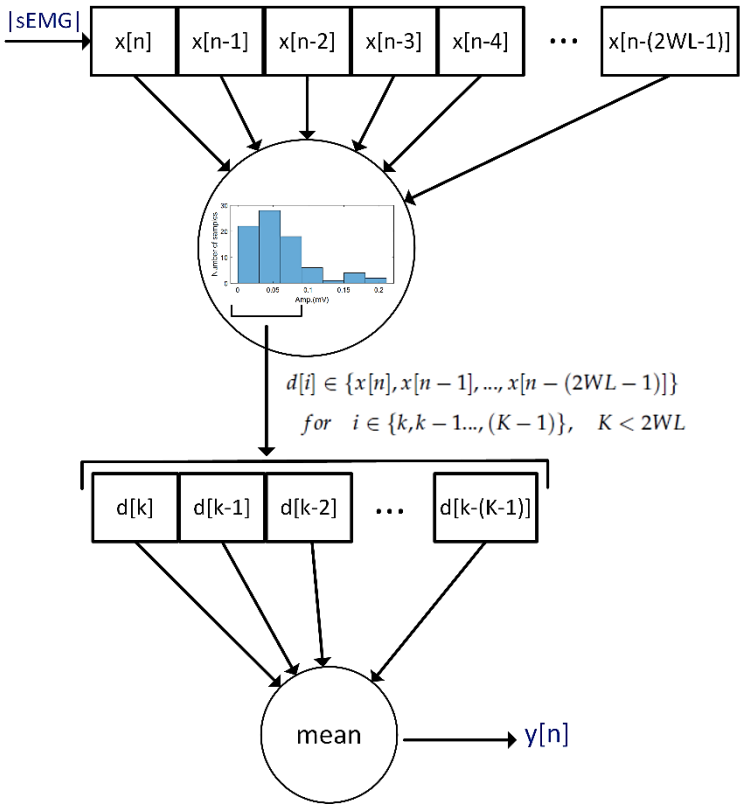

Figure 2. The principle of the operation of MAHF. The seven-bin histogram of the sEMG data contained in the window (X = {x[n], x[n − 1], ... x[n − (2WL − 1)]}) of 2WL length is calculated. Next, the vector D of sEMG samples d[i], for i ∈ {k, k – 1 ..., (K − 1)}, where K < 2WL, belonging to the three most numerous bins, is created. The mean value of D is the output of the filter.

Next, the signals were processed using an RMS window length of 150 ms (Burden et al., 2014). The kurtosis parameter was used to assess the influence of the proposed filtering method on sEMG signal. Next, by determining the threshold value of the sEMG signal, the level of muscle excitation was determined.

2.2. Kurtosis

According to the literature (Michell, 2013), more motor unit action potentials are fired with increasing the force level during contraction. Because the sEMG signal is the superposition of these potentials, it tends to be a Gaussian process at high force levels (Nazarpour et al., 2005, 2013). In this research, kurtosis was used to evaluate the Gaussianity of sEMG signals. Kurtosis (1) is a classic method of measuring non-Gaussianity (Hyvärinen, Oja, 2000). It is a measure of the sensitivity of the distribution to outliers. In classic terms, kurtosis is expressed by (1) (Hyvärinen and Oja, 2000):

$$kurt(s) = E\{s^4\} - 3(E\{s^2\})^2, \tag{1}$$

where s is a signal and E{s} is expected value of the signal s. In our study to calculate the kurtosis of a discrete sEMG signal, the following formula (2) is used:

$$kurt(s) = \frac{\frac{1}{N}\sum_{i=1}^{N}(x_i-\mu)^4}{\left(\frac{1}{N}\sum_{i=1}^{N}(x_i-\mu)^2\right)^2}, \tag{2}$$

where μ is the mean of the discrete signal s = [x_1, x_2, ..., x_N] and N is the number of signal samples. Kurtosis for the Gaussian random variable (s) calculated according to the formula (2) is equal to 3.

2.3. Thresholding

Threshold calculation is performed on sEMG intervals presenting muscle excitation split into 100 ms segments. In the first step, the level of artifacts is found. To gain insight into the rate of amplitude changes, for each segment, the first derivative is calculated, and the variance of the derivative is determined (variance is the measure of dispersion). Then, the mean (MD) and standard deviation values (STDD) of variance from the segments of derivatives are calculated by (3) and (4), respectively.

$$MD = \frac{1}{N}\sum_{i=1}^{N} v_i, \tag{3}$$

$$STDD = \sqrt{\sum_{i=1}^{N}\frac{(v_i-MD)^2}{N}}, \tag{4}$$

where v_i denotes the variance of derivatives of i-th segments of sEMG signal for all (N) sEMG segments under consideration. The threshold level for detecting artifacts (TAL) is determined using the following formula:

$$TAL = MD + sl \cdot STDD, \tag{5}$$

where MD (3) and STDD (4) are the mean and standard deviation (Kabe and Sako, 2020) of variance from the segments of derivatives, respectively, and sl is a constant that determines the

sensitivity of artifacts detection. In our case, it was set to 0.95. In the second step, the variance value of each segment is compared with TAL. If the variance of the first derivative of a given segment exceeds the TAL value, the analyzed segment of the sEMG signal is marked as noisy. Next, the maximum amplitude of the sEMG signal is determined (MA) according to:

$$A\big(x(n)\big) = \underset{i\in\{1,2,\dots K\}}{max}\, x(i), \tag{6}$$

where x(n) is discrete sEMG signal and K denotes the length of analyzed sEMG (not noisy marked).

Segments marked as noisy are omitted when determining the maximum amplitude. Then, samples of the sEMG signal exceeding the maximum are dropped. The maximum value and time location are searched in the sEMG signal prepared in this way. In the last step, a 2D (D = 50 ms) length window was created relative to the determined position. The threshold value was defined as the mean of the sEMG signal in the assumed window and refers to the level of muscle excitation. The illustration of the threshold operation is shown in Figure 3.

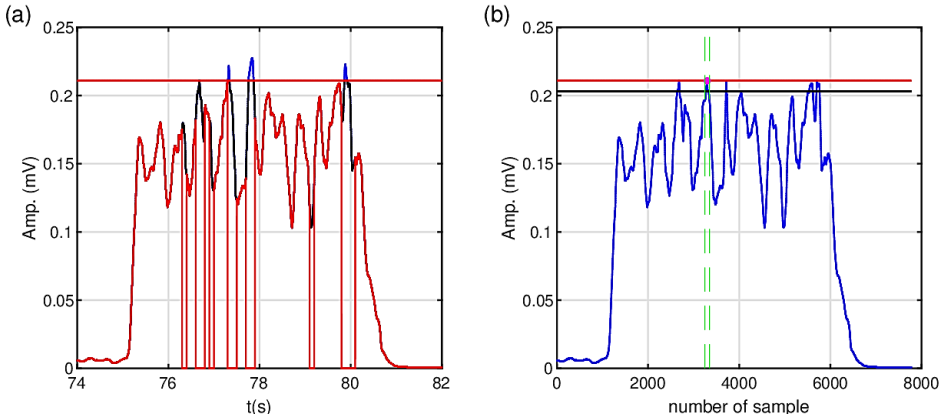

Figure 3. Illustration of the threshold operation; analyzed fragment of sMEG (red), noised segment (black), MA (horizontal red dashed line), spikes excluded from threshold analysis (blue) (a); sEMG after removing spikes (blue), MA (horizontal red line), level of muscle excitation determined (horizontal black line), 2D (100 ms) length window (vertical green dashed lines) for determining level of muscle excitation (b).

3. Results

The operation of the proposed method is illustrated in Figures 4-7. An example of a raw sEMG signal recorded for the normalization process (MVC estimation) of the left rectus femoris muscle during two repetitions is depicted in Figure 4.

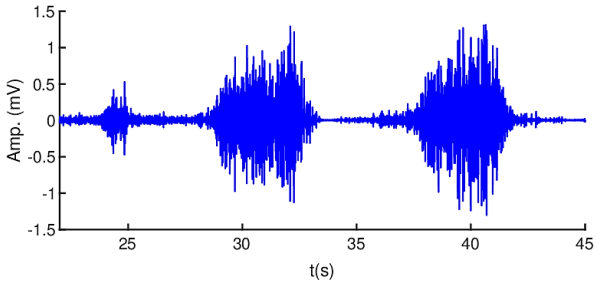

Figure 4. An example of raw sEMG signal recorded for normalization process from left rectus femoris muscle during two repetitions.

Figure 5 shows the filtered (by HPF, LPF and BSF), rectified samples of raw sEMG versus the sEMG signal processed by the proposed method.

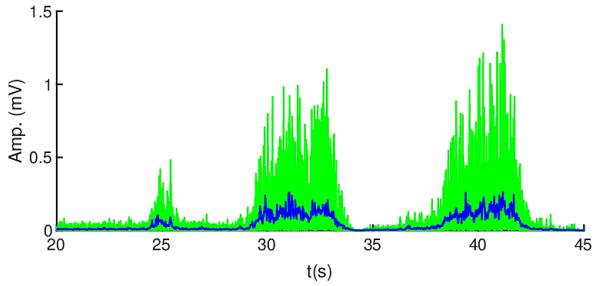

Figure 5. An example of the absolute value of filtered (by HPF, LPF and BSF) rectified sEMG signal (green) and sEMG after filtering by MAH filter (blue).

Figure 6 shows the comparison of the RMS values of the sEMG signal obtained by the standard and proposed method.

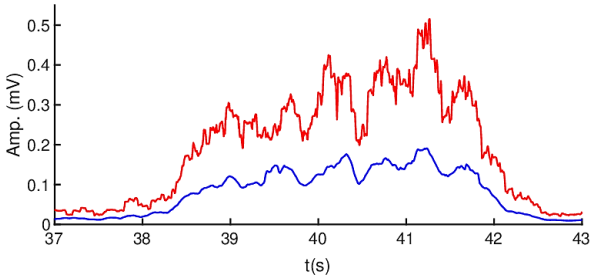

Figure 6. Comparison of RMS values of sEMG obtained by classic (red line) and proposed method (blue line).

Figure 7 presents both the calculated MVC level by the proposed method and the maximum value of the sEMG amplitude. Figure 8 shows the RMS values of the sEMG signal for normalization and the calculated MVC levels obtained by the classic and proposed method in the second repetition, while Figure 9 shows the RMS values of sEMG signal and the determined level of vastus medialis excitation in the deep squat calculated by the classic and proposed method.

Kurtosis of the sEMG fragment was estimated for each repetition before and after preprocessing to determine the MVC level. For the first repetition of the normalization exercise, kurtosis was equal to 4.16 and 3.30, before and after preprocessing, respectively, and 5.59 and 2.92 for the second repetition. As the sEMG signal distribution for the MVC estimation should tend to a normal distribution, the second repetition after preprocessing with kurtosis equal to 2.92 was taken into further analysis.

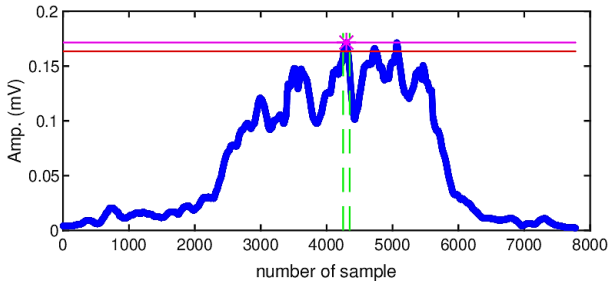

Figure 7. Determination of MVC level. The maximum amplitude of the sEMG signal is marked by a *sign and a line in magenta color, and a red line marks the MVC level determined by the proposed method. The sampling frequency is equal to 1000 Hz.

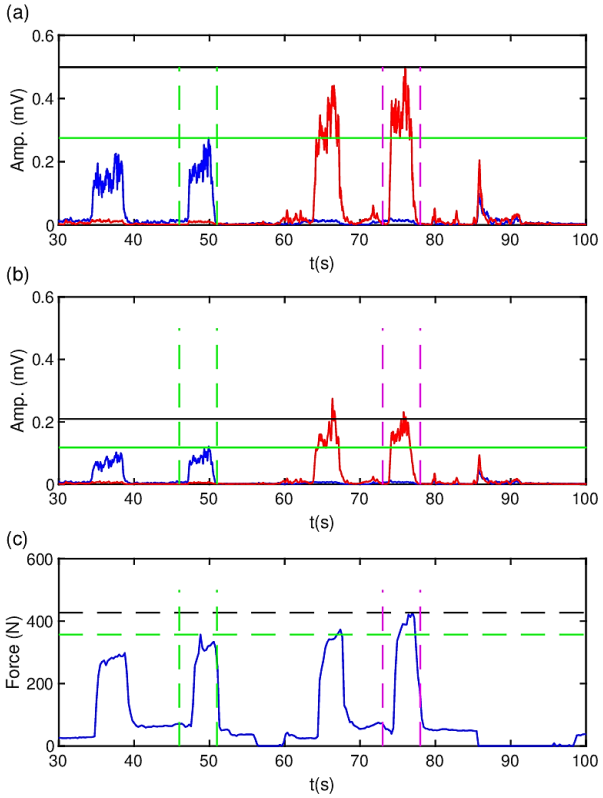

Figure 8. Example of MVC determination levels for RMS obtained by the classic (a) and proposed method (b) for left (blue line) and right (red line) vastus medialis. A horizontal line marks the MVC for the second repetition in green for the left muscle and black for the right muscle. Additionally, the corresponding values of measured force are presented (c).

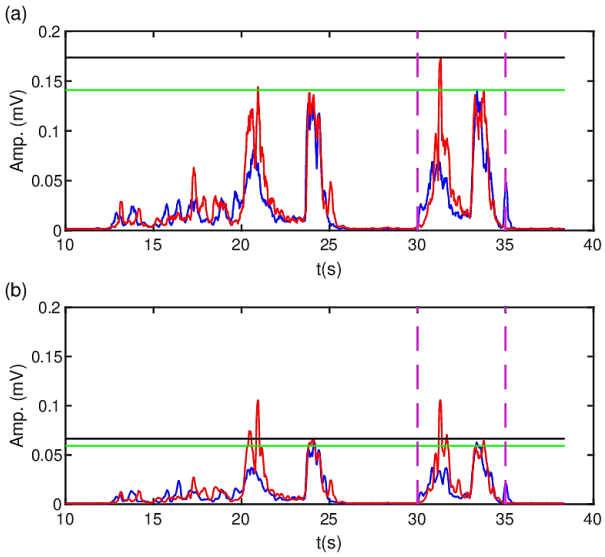

Figure 9. Example of determined levels of vastus medialis excitation in deep squat calculated for RMS obtained by classic (a) and the proposed method (b) for left (blue line) and right (red line) vastus medialis. A horizontal line marks the MVC for the second repetition in green for the left muscle and in black for the right muscle.

The results of maximum excitation expressed in %MVC for the left and right rectus femoris, vastus medialis, and biceps femoris muscles for the classic and proposed method during deep squat activity are summarized in tables 1-2 and 3-4, respectively. Based on analyzed sEMG signals and level of muscle excitation, the outcomes obtained were divided into two groups. The main factor that suggested the division into groups was the difference in the level of excitation in the biceps femoris. Tables 1, 3 and 2, 4 show the results for groups 1 and 2 for both the classic and proposed methods.

In addition, the excitation levels of the rectus femoris, vastus medialis, and biceps femoris for each group and each person (for the left and right muscle separately) are illustrated in Figures 10-11 (classic method) and 12-13 (proposed method).

Table 1.
The results (classic method) of maximum excitation in %MVC for left and right rectus femoris, vastus medialis and biceps femoris muscle during deep squat activity for group 1

Person	Muscle	Rectus Femoris %MVC	Vastus Medialis %MVC	Biceps Femoris %MVC
1	Left	62	58	10
	Right	79	65	5
2	Left	68	29	3
	Right	49	30	3
3	Left	85	76	16
	Right	124	42	11
4	Left	21	49	11
	Right	34	59	12

Table 2.
The results (classic method) of maximum excitation in %MVC for left and right rectus femoris, vastus medialis and biceps femoris muscle during deep squat activity for group 2

Person	Muscle	Rectus Femoris %MVC	Vastus Medialis %MVC	Biceps Femoris %MVC
5	Left	15	66	31
	Right	31	50	8
6	Left	54	68	3
	Right	63	109	25
7	Left	63	45	62
	Right	51	85	12
8	Left	12	38	75
	Right	59	37	24

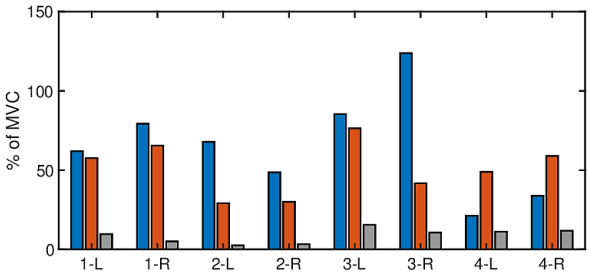

Figure 10. The results (classic method) of maximum excitation expressed in %MVC for left and right rectus femoris (blue bar), vastus medialis (red bar) and biceps femoris (gray bar) muscle during deep squat activity for group 1.

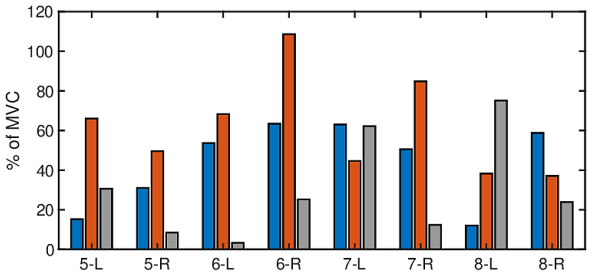

Figure 11 The results (classic method) of maximum excitation expressed in %MVC for left and right rectus femoris (blue bar), vastus medialis (red bar) and biceps femoris (gray bar) muscle during deep squat activity for group 2.

Table 3.
The results (proposed method) of maximum excitation in %MVC for left and right rectus femoris, vastus medialis and biceps femoris muscle during deep squat activity for group 1

Person	Muscle	Rectus Femoris %MVC	Vastus Medialis %MVC	Biceps Femoris %MVC
1	Left	48	51	7
	Right	37	51	5
2	Left	77	34	2
	Right	38	40	3
3	Left	92	93	12
	Right	126	45	14
4	Left	23	47	13
	Right	29	58	9

Table 4.
The results (proposed method) of maximum excitation in %MVC for left and right rectus femoris, vastus medialis and biceps femoris muscle during deep squat activity for group 2

Person	Muscle	Rectus Femoris %MVC	Vastus Medialis %MVC	Biceps Femoris %MVC
5	Left	13	67	15
	Right	26	32	4
6	Left	69	58	3
	Right	57	86	21
7	Left	60	55	66
	Right	32	64	11
8	Left	14	69	77
	Right	30	41	17

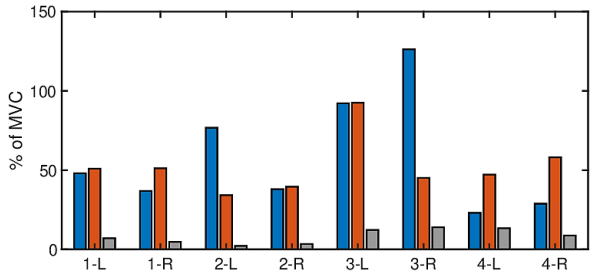

Figure 12. The results (proposed method) of maximum excitation expressed in %MVC for left and right rectus femoris (blue bar), vastus medialis (red bar) and biceps femoris (gray bar) muscle during deep squat activity for group 1.

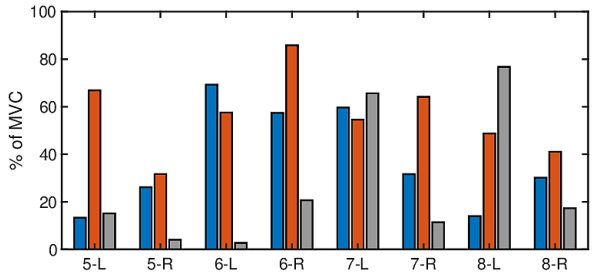

Figure 13. The results (proposed method) of maximum excitation expressed in %MVC for left and right rectus femoris (blue bar), vastus medialis (red bar) and biceps femoris (gray bar) muscle during deep squat activity for group 2.

3.1. Statistical Analysis

In the first step of the statistical analysis, the consistency of the results obtained by the methods considered: classic and proposed was validated. The normal distribution of data (for whole data and separately for data obtained with the classic and proposed method) were tested by the Lilliefors-Corrected Kolmogorov-Smirnov test because of the not known expected value and variance for the whole population. In general, the data examined were not normal distributed (for the rectus femoris, vastus medialis $p > 0.2$ and biceps femoris $p < 0.05$), therefore the nonparametric (independent of the distribution of random variable) Mann-Whitney U test was performed. Based on the non-parametric Mann-Whitney U test, it was shown that the null hypothesis that randomly selected samples came from populations

with equal medians could not be rejected (p =0.44 for rectus femoris, p = 0.87 for vastus medialis, and p = 0.79 for biceps femoris), which would indicate the consistency of the results obtained for individual methods. Analyzing the box plots (Figure 14) of muscles excitation during deep squat for the classic and the proposed method, it could be noticed a decrease in the dispersion of excitation values for vastus medialis in the case of the proposed method.

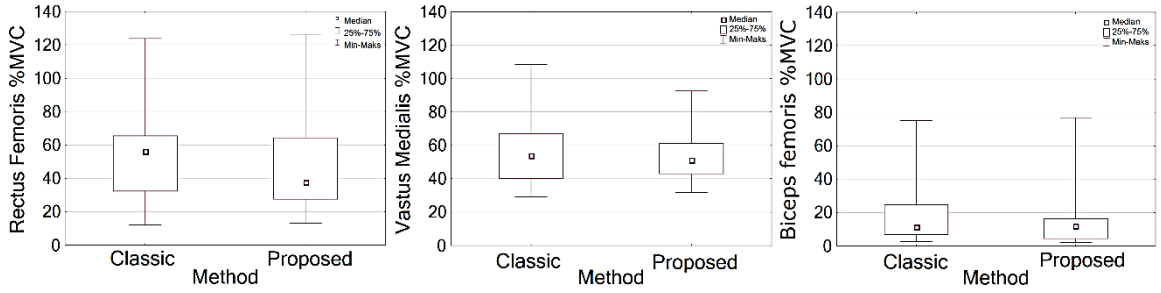

Figure 14. Box plots of rectus femoris, vastus medialis and biceps femoris muscles excitation levels for classic and proposed methods.

Box plots in Figure 15 show the relationship between the excitation of individual muscles in groups 1 and 2, depending on the method used.

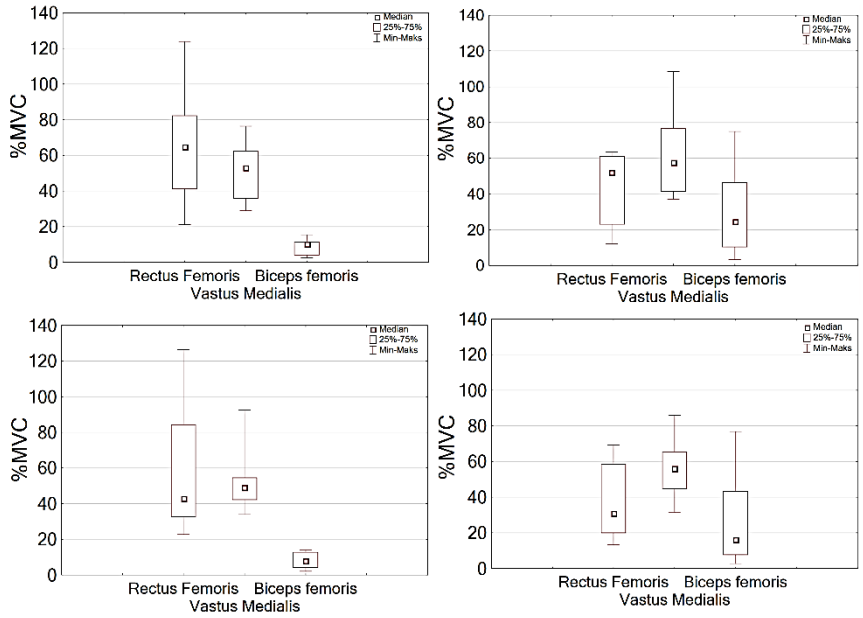

Figure 15. Box plots of rectus femoris, vastus medialis, and biceps femoris muscles excitation levels obtained for the classic (in the top) and the proposed (in the bottom) methods. Results for groups 1 and 2 are presented on the left and right columns, respectively.

4. Discussion

The presented work proposes an sEMG signal processing method to determine the value of muscle excitation, which relates to muscle contraction. The described method can be used to assess motor control strategy, that is, muscles contribution to particular physical activity. The main motivation for proposing this method of sEMG signal processing was the need to eliminate impulse interference (narrow spikes) from the sEMG signal. The common cause of these artifacts is both the EMG signal's nature and its recording technique (e.g., use of surface electrodes, recording during movements) (Qiu et al., 2015; Boyer et al., 2023). Narrow spikes appearing in the sEMG signal might significantly influence the correctness of the classic method of estimating muscle excitation, mainly because these disturbances are often of great amplitude and interfere with the maximum value of amplitude taken into account in the classic method (Konrad, 2005; Josephson, Knight, 2019).

The healthy relaxed muscle produces no significant excitation due to the lack of depolarization and repolarization of the sarcolemma of muscle fiber, that is, the lack of action potentials. Appearing action potentials recorded in a raw sEMG are randomly shaped spikes because the actual set of recruited motor units is constantly changing (Cavalcanti Garcia, Vieira, 2011), so they also change their diameters and distances from the electrodes. Suppose some motor units in the close neighborhood are recruited at the same time. In that case, the generated action potentials superimpose, and if the motor units are additionally located near the electrode, a significant spike may be observed in the raw sEMG (Roeleveld et al., 2003).

The reason is that the sEMG signal is usually recorded during physical activity, which results, for example, in the problem of ensuring proper electrode-skin contact (Yeon, Herr, 2021). Temporary loss of electrode contact may also cause disturbances (Olmo, Domingo, 2020), which, if not eliminated, may significantly affect the determination of some parameters of the sEMG signal (e.g., the value of maximum excitation, which reflects maximum muscle contraction). The proposed algorithm attenuates disturbances both at the stage of sEMG signal preprocessing and at the stage of determining the maximum value of muscle excitation (thresholding). The exemplary outcomes of the proposed sEMG signal processing method, presented in the results section, show the effectiveness of eliminating impulse interference at the filtering stage and during determining the level of muscle excitation.

It can be noticed that the presented method affects the amplitude of the processed sEMG signal compared to the classic method. However, it does not affect the calculated normalized muscle excitation level as long as the normalization process (Chalard et al., 2020; Halaki, Ginn, 2012) is correct and the normalized and normalizing signals are processed using the same (proposed) method. The comparison of kurtosis for raw signals and signals processed with the proposed method shows that the method minimizes too aggressive filtering of the sEMG signal. In the case of the analyzed fragments of sEMG signals in the interval where MVC was

determined, the post-filtering signal distribution was close to normal, with kurtosis of about three.

Performed statistical analysis did not point out the significant differences between the outcomes obtained by the classic and proposed method in terms of maximal excitation of the rectus femoris, vastus medialis, and biceps femoris muscles in the deep squat. Both methods give consistent results, especially for good-quality sEMG signals. The problem arises when the impulse interference appears in the sEMG recording and has not been eliminated by the RMS method, which can be observed in Figure 8, in such cases, the proposed method gives better results (Figure 14 (for vastus medialis)), and the estimated maximum excitation seems to be closer to that of physiological origin.

According to the assessment of physiotherapists, the main active muscles in the deep squat are the rectus femoris and the vastus medialis, while the biceps femoris was rated as weakly active or even inactive in this exercise. Analysis of the muscle excitation values for the deep squat using both the classic and proposed methods allowed to distinguish two groups of athletes depending on the excitation of the biceps femoris muscle.

For group 1 the excitation of the biceps femoris does not exceed 16%MVC (mean = 8.70, std = 4.58, stderror = 1.62) in the classic method and 14%MVC (mean = 8.20, std = 4.61, stderror = 1.63) in the proposed method, therefore, the excitation of the biceps femoris is low enough to confirm the suggestion of the physiotherapists that in the deep squat the excitation of the biceps femoris is at a low level with the dominant excitation of the vastus medialis and rectus femoris. The results obtained (Figures 10, 12) show that this tendency is maintained for both the left and right muscles.

In the case of group 2, both methods indicate a decrease in the rectus femoris excitation by an average of approximately 21%MVC compared to group 1, while increasing biceps femoris excitation by more than 21.46%MVC (compared to group 1) in the classic method and 18.51%MVC in the proposed method. For the vastus medialis, the classic method showed a decrease in excitation of about 11.14%MVC in relation to group 1, while the proposed method showed an increase in excitation of about 14.56%MVC. The observed effect of activation of the biceps femoris muscle may result from a limited range of motion in the ankle joint or too little flexibility of the posterior muscle band. Activation of the antagonist's muscle may indicate that the person performing the exercise was trying to compensate, for example, for the tendency to valgus the knee resulting from the above limitations. Differences in the assessment of the excitation of the vastus medialis muscle using the classic method and the proposed method probably result from artifacts disturbing the maximum value of the amplitude in the sEMG signals (Figures 9, 14 (for the vastus medialis)).

Correctly evaluating individual muscle excitation for a given exercise can provide a deeper insight into how the muscles work during this exercise and can also be used to assess progress during training or rehabilitation. The emerging disproportion in muscle excitation can be both a remnant of a past injury and a harbinger of an injury in the future. In the future, enlarging

group 1 with a larger number of athletes, for whom the muscles excitation (active muscles: rectus femoris and vastus medialis) would be assessed by both the classic and proposed method, could allow for definite the ranges of excitation for considered muscles in the case of a properly performed exercise. The excitation ranges obtained could be the reference values for assessing any athlete's muscle condition in the deep squat. The limitation and disadvantage of the proposed method may be that in some cases, due to the nature of the sEMG or EMG signal, which is random and non-stationary, part of the signal may be treated as an impulse disturbance. Therefore, the proposed method should not be used during studies concerned with the analysis of single muscle fiber excitation, which may be in the form of short pulses of high amplitude, is important. Also, depending on the sEMG signal recording parameters, for example, the value of sampling frequency, some parameters of the proposed method, such as the number of histogram bins used in the proposed FMAH filter, may need to be changed.

5. Conclusions

The determination of proper muscle excitation requires preprocessing and normalization of the sEMG signal. The selection of the normalizing exercise, as well as the careful execution of this exercise, are of great importance for the normalization process and muscle excitation estimation. The proposed approach for sEMG analysis provides an effective method for assessing muscle excitation during sports activity. The combination of the MAHF filter and the analysis variance-based thresholding method can effectively eliminate impulse artifacts (pulse with high amplitude, e.g., caused by electrode contact variation) within the sEMG signals, which makes the determined level of muscle excitation more reliable. The results of preliminary studies are promising because they seem to be closer to that of physiological origin and consistent with the suggestions of physiotherapists. The proposed method was also developed to reduce computational complexity and to be easily applied to online sEMG analysis.

Contributions

The authors participated in all activities that contributed to the writing of this article. All authors have read and approved the final version of the manuscript, and agree with the order of presentation of the authors.

Funding

This research was funded by the Silesian University of Technology. The data collection process was funded by the Polish National Center for Research and Development grant number POIR.01.01.01-00-0653/19.

Conflicts of Interest

The authors declare that they have no competing interests. Informed Consent Statement: Informed consent was obtained from all subjects involved in the study.

Abbreviations

The following abbreviations are used in this manuscript:

BMI	Body Mass Index
BN	Number of Bins
BSF	Band Stop Filter
CMS	Central Nervous System
CP	Cut-off Point
EMG	Electromyographical signal
FIR	Finite Impulse Response Filter
HPF	High Pass Filter
iEMG	Intra-Muscular Electromyographical Signal
LPF	Low Pass Filter
MA	Maximum Amplitude of the sEMG Signal
MAHF	Moving Average Hole Filter
MD	Mean of Variance from the Segments of Derivatives
MVC	Maximum Voluntary Contraction
MUAPs	Motor Unit Action Potentials
RMS	Root Mean Square
SENIAM	Surface Electromyography for the Non-Invasive Assessment of Muscles
sEMG	Surface Electromyographical Signal
STDD	Standard Deviation of Variance from the Segments of Derivatives
WL	Window Length

References

1. Arabadzhiev, T.I., Dimitrov, V.G., Dimitrova, N.A., Dimitrov, G.V. (2010). Interpretation of EMG integral or RMS and estimates of "neuromuscular efficiency" can be misleading in fatiguing contraction. *Journal of Electromyography and Kinesiology, 20,* 223–232, https://doi.org/https://doi.org/10.1016/j.jelekin.2009.01.008.
2. Arozi, M., Ariyanto, M., Kristianto, A., Munadi., Setiawan, J.D. (2020). *EMG Signal Processing of Myo Armband Sensor for Prosthetic Hand Input using RMS and ANFIS.* Proceedings of the 7th International Conference on Information Technology, Computer, and Electrical Engineering (ICITACEE), pp. 36–40, https://doi.org/10.1109/ ICITACEE50144.2020.9239169.
3. Boyer, M., Bouyer, L., Roy, J.S., Campeau-Lecours, A. (2023). Reducing Noise, Artifacts and Interference in Single-Channel EMG Signals: A Review. *Sensors, 23,* 2927, https://doi.org/10.3390/s23062927.
4. Burden, M.A., Lewis, S.E., Willcox, E. (2014). The effect of manipulating root mean square window length and overlap on reliability, inter-individual variability, statistical significance and clinical relevance of electromyograms. *Manual Therapy, 19,* 595–601, https://doi.org/10.1016/j.math.2014.06.003.
5. Calderón, J.C., Bolaños, P., Caputo, C. (2014). The excitation–contraction coupling mechanism in skeletal muscle. *Biophysical Reviews, 6,* 133–160, https://doi.org/10.1007/s12551-013-0135-x.
6. Cavalcanti Garcia, M.A., Vieira, T. (2011). Surface electromyography: Why, when and how to use it. *Revista Andaluza de Medicina del Deporte, 4,* 17–28.
7. Chalard, A., Belle, M., Montané, E., Marque, P., Amarantini, D., Gasq, D. (2020). Impact of the EMG normalization method on muscle activation and the antagonist-agonist co-contraction index during active elbow extension: Practical implications for post-stroke subjects. *Journal of Electromyography and Kinesiology, 51,* 102403, https://doi.org/https://doi.org/10.1016/j.jelekin.2020.102403.
8. Chmielewska, D., Stania, M., Kucab-Klich, K., Błaszczak, E., Kwaśna, K., Smykla, A., Hudziak, D., Dolibog, P. (2019). Electromyographic characteristics of pelvic floor muscles in women with stress urinary incontinence following sEMG-assisted biofeedback training and Pilates exercises. *PloS One, 14(12),* https://doi.org/https://doi.org/10.1371/journal. pone.0225647.
9. Chowdhury, R., Reaz, M., Ali, M., Bakar, A., Chellappan, K., Chang, T. (2013). Surface Electromyography Signal Processing and Classification Techniques. *Sensors, 13,* 12431–12466, https://doi.org/10.3390/s130912431.

10. De Luca, C.J. (1997). Physiology and Mathematics of Myoelectric Signals. *IEEE Transactions on Biomedical Engineering, BME-26,* 313–325, https://doi.org/10.1109/TBME.1979.326534.
11. De Luca, C.J., Donald Gilmore, L., Kuznetsov, M., Roy, S.H. (2010). Filtering the surface EMG signal: Movement artifact and baseline noise contamination. *Journal of Biomechanics, 43,* 1573–1579, https://doi.org/10.1016/j.jbiomech.2010.01.027.
12. Dulhunty, A.F. (2006). Excitation–Contraction Coupling From the 1950s Into the New Millennium. *Clinical and Experimental Pharmacology and Physiology, 33,* 763–772, https://doi.org/10.1111/j.1440-1681.2006.04441.x.
13. Farina, D., Fosci, M., Merletti, R. (2002). Motor unit recruitment strategies investigated by surface EMG variables. *Journal of Applied Physiology, 92,* 235–247, https://doi.org/10.1152/jappl.2002.92.1.235.
14. Farina, D., Stegeman, D.F., Merletti, R. (2016). *Biophysics of the Generation of EMG Signals.* pp. 1-24. https://doi.org/https: //doi.org/10.1002/9781119082934.ch02.
15. Freriks, B., Hermens, H. (1999). *SENIAM 9: European Recommendations for Surface Electromyography, results of the SENIAM project*. Roessingh Research and Development.
16. Gupta, A., Sayed, T., Garg, R., Shreyam, R. (2017). Emg Signal Analysis of Healthy and Neuropathic Individuals. *IOP Conference Series: Materials Science and Engineering, 225,* 012128, https://doi.org/10.1088/1757-899X/225/1/012128.
17. Halaki, M., Ginn, K., (2012). *Normalization of EMG Signals: To Normalize or Not to Normalize and What to Normalize to?*, pp.175–194, https://doi.org/10.5772/49957.
18. Hermens, H., Freriks, B., Merletti, R., Hägg, G., Stegeman, D.F., Blok, J., Rau, G., Disselhorst-Klug, C. (1999). *SENIAM 8: European Recommendations for Surface ElectroMyoGraphy*. Roessingh Research and Development.
19. Hyvärinen, A., Oja, E. (2000). Independent component analysis: algorithms and applications. *Neural Networks, 13,* 411–430, https://doi.org/https://doi.org/10.1016/S0893-6080(00)00026-5.
20. Jórasz, K., Truszczyńska-Baszak, A., Dabek, A. (2023). Posture Correction Therapy and Pelvic Floor Muscle Function Assessed by sEMG with Intravaginal Electrode and Manometry in Female with Urinary Incontinence. *International Journal of Environmental Research and Public Health, 20*. https://doi.org/10.3390/ijerph20010369.
21. Josephson, M.D., Knight, C.A. (2019). Comparison of neural excitation measures from the surface electromyogram during rate-dependent muscle contractions. *Journal of Electromyography and Kinesiology, 44,* 15–20, https://doi.org/https://doi.org/10.1016/j.jelekin.2018.11.004.
22. Kabe, A.M., Sako, B.H. (2020). Chapter 5 - Analysis of continuous and discrete time signals. In: A.M. Kabe, B.H. Sako (Eds.), *Structural Dynamics Fundamentals and Advanced Applications.* Academic Press, pp. 271–427, https://doi.org/https://doi.org/10.1016/B978-0-12-821615-6.00005-8.

23. Karabulut, D., Ortes, F., Arslan, Y.Z., Adli, M.A. (2017). Comparative evaluation of EMG signal features for myoelectric controlled human arm prosthetics. *Biocybernetics and Biomedical Engineering, 37,* 326–335, https://doi.org/https://doi.org/10.1016/j.bbe.2017.03.001.
24. Konrad, P. (2005). *The ABC of EMG: A practical introduction to kinesiological electromyography, version 1.0 ed*. USA: Noraxon INC.
25. Luca, C.J.D. (1997). The Use of Surface Electromyography in Biomechanics. *Journal of Applied Biomechanics, 13*, 135 – 163, https://doi.org/10.1123/jab.13.2.135.
26. Martín, C., Palma, J.C., Alamán, J.M., Lopez-Quiñones, J.M., Alarcón, J.A. (2012). Longitudinal evaluation of sEMG of masticatory muscles and kinematics of mandible changes in children treated for unilateral cross-bite. *Journal of Electromyography and Kinesiology, 22,* 620–628, https://doi.org/https://doi.org/10.1016/j.jelekin.2012.01.002.
27. Merletti, R., Parker, P. (eds.), (2004). *Electromyography: Physiology, Engineering, and Non-Invasive Applications.* John Wiley & Sons, Inc.
28. Michell, A. (2013). *Understanding EMG*. Oxford University Press, https://doi.org/10.1093/med/9780199595501.001.0001.
29. Moritani, T., Stegeman, D., Merletti, R. (2004). Basic Physiology and Biophysics of EMG Signal Generation. In: R. Merletti, P. Parker (Eds.), *Electromyography* (pp. 1-25); JohnWiley & Sons, https://doi.org/10.1002/0471678384.ch1.
30. Nazarpour, K., Al-Timemy, A.H., Bugmann, G., Jackson, A. (2013). A note on the probability distribution function of the surface electromyogram signal. *Brain Research Bulletin, 90,* 88–91, https://doi.org/10.1016/j.brainresbull.2012.09.012.
31. Nazarpour, K., Sharafat, A.R., Firoozabadi, S.M. (2005). Negentropy analysis of surface electromyogram signal. *IEEE*, https: //doi.org/10.1109/ssp.2005.1628736.
32. Olmo, M.D., Domingo, R. (2020). EMG Characterization and Processing in Production Engineering. *Materials, 13,* 5815. https://doi.org/10.3390/ma13245815.
33. Pilkar, R., Momeni, K., Ramanujam, A., Ravi, M., Garbarini, E., Forrest, G.F. (2020). Use of Surface EMG in Clinical Rehabilitation of Individuals With SCI: Barriers and Future Considerations. *Frontiers in Neurology, 11*, https://doi.org/10.3389/fneur.2020.578559.
34. Qiu, S., Feng, J., Xu, R., Xu, J., Wang, K., He, F., Qi, H., Zhao, X., Zhou, P., Zhang, L. et al. (2015). A Stimulus Artifact Removal Technique for SEMG Signal Processing During Functional Electrical Stimulation. *IEEE Transactions on Biomedical Engineering, 62,* 1959–1968, https://doi.org/10.1109/TBME.2015.2407834.
35. Reaz, M.B.I., Hussain, M.S., Mohd-Yasin, F. (2006). Techniques of EMG signal analysis: Detection, processing, classification and applications. *Biological Procedures Online, 8,* 11–35, https://doi.org/10.1251/bpo115.
36. Rodríguez-Carreño, I., Gila-Useros, L., Malanda-Trigueros, A. (2012). Motor Unit Action Potential Duration: Measurement and Significance: 7. In: I.M. Ajeena (Ed.), *Advances in Clinical Neurophysiology.* Rijeka: IntechOpen, https://doi.org/10.5772/50265.

37. Roeleveld, K., Stegeman, D.F., Vingerhoets, H.M., Van Oosterom, A. (2003). The motor unit potential distribution over the skin surface and its use in estimating the motor unit location. *Acta Physiologica Scandinavica, 161,* 465–472. https://doi.org/10.1046/j.13 65-201X.1997.00247.x.
38. Rose, W. (2014). *Electromyogram analysis. Mathematics and Signal Processing for Biomechanics.* Delaware.
39. Sadikoglu, F., Kavalcioglu, C., Dagman, B. (2017). Electromyogram (EMG) signal detection, classification of EMG signals and diagnosis of neuropathy muscle disease. *Procedia Computer Science, 120,* 422–429, https://doi.org/10.1016/j.procs.2017.11.259.
40. Sarillee, M., Hariharan, M., Anas, M.N., Omar, M.I., Aishah, M.N., Oung, Q. (2014). *Non-invasive techniques to assess muscle fatigue using biosensors: A rev*iew. Proceedings of the IEEE 5th Control and System Graduate Research Colloquium, pp. 187–192, https://doi.org/10.1109/ICSGRC.2014.6908719.
41. Smith., S.W. (1997-1998). *The Scientist and Engineer's Guide to Digital Signal Processing*.
42. Staudenmann, D., Roeleveld, K., Stegeman, D.F., van Dieën, J.H. (2010). Methodological aspects of SEMG recordings for force estimation – A tutorial and review. *Journal of Electromyography and Kinesiology, 20,* 375–387. https://doi.org/https: //doi.org/10.1016/j.jelekin.2009.08.005.
43. Stegeman, D., Hermens, H. (2007). *Standards for surface electromyography: The European project Surface EMG for non-invasive assessment of muscles (SENIAM) 2007. 1*.
44. Sun, J., Liu, G., Sun, Y., Lin, K., Zhou, Z., Cai, J. (2022). Application of Surface Electromyography in Exercise Fatigue: A Review. *Frontiers in Systems Neuroscience, 16,* https://doi.org/10.3389/fnsys.2022.893275.
45. Trontelj, J.V., Jabre, J., Mihelin, M. (2004). Needle and Wire Detection Techniques. In: R. Merletti, P. Parker (Eds), *Electromyography* (pp. 27–46). John Wiley & Sons. https://doi.org/10.1002/0471678384.ch2.
46. Vigotsky, A.D., Halperin, I., Lehman, G.J., Trajano, G.S., Vieira, T.M. (2018). Interpreting Signal Amplitudes in Surface Electromyography Studies in Sport and Rehabilitation Sciences. *Frontiers in Physiology*, https://doi.org/10.3389/fphys.2017.00985.
47. Wang, M.Q., He, J.J., Zhang, J.H., Wang, K., Svensson, P., Widmalm, S.E. (2010). SEMG activity of jaw-closing muscles during biting with different unilateral occlusal supports. *Journal of oral rehabilitation, 37, 9,* 719–25.
48. Xu, L., Gu, H., Zhang, Y. (2022). Research Hotspots of the Rehabilitation Medicine Use of sEMG in Recent 12 Years: A Bibliometric Analysis. *Journal of Pain Research, Vol. 15,* 1365–1377, https://doi.org/10.2147/JPR.S364977.
49. Yeon, S.H., Herr, H.M. (2021). *Rejecting Impulse Artifacts from Surface EMG Signals using Real-time Cumulative Histogram Filtering*. Proceedings of the 43rd Annual International Conference of the IEEE Engineering in Medicine & Biology Society (EMBC), pp. 6235–6241, https://doi.org/10.1109/EMBC46164.2021.9631052.

50. Yin, G., Zhang, X., Chen, D., Li, H., Chen, J., Chen, C., Lemos, S. (2020). Processing Surface EMG Signals for Exoskeleton Motion Control. *Frontiers in Neurorobotics, 14*, 118, https://doi.org/10.3389/fnbot.2020.00040.
51. Zajac, F.E. (1989). Muscle and tendon: properties, models, scaling, and application to biomechanics and motor control. *Critical reviews in biomedical engineering, 17, 4,* 359–411.
52. Zieliński, G., Baszczowski, M., Rapa, M. et al. (2022b). The Axial Length of the Eyeball and Bioelectrical Activity of Masticatory and Neck Muscles: A Preliminary Report. *Pain Res. Manag., 6115782*, https://doi.org/10.1155/2022/6115782.
53. Zieliński, G., Matysik-Woźniak, A., Baszczowski, M. et al. (2022a). Effects of visual input on changes in the bioelectrical activity of the cervical and masticatory muscles in myopic subjects. *Sci. Rep., 12, 9435*. https://doi.org/https://doi.org/10.1038/s41598-022-13607-1.
54. Zwarts, M., Stegeman, D., van Dijk, J. (2004). *Surface EMG applications in neurology*. IEEE Press Editorial Board, p. 323.